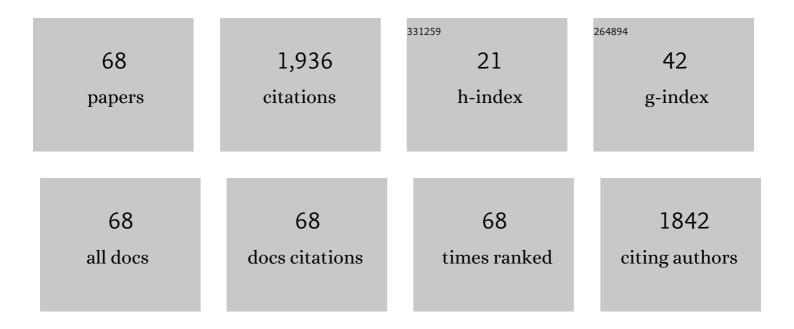
Shengcheng Mao

List of Publications by Year in descending order

Source: https://exaly.com/author-pdf/3116235/publications.pdf Version: 2024-02-01



#	Article	IF	CITATIONS
1	Effects of the orientation relationships between TCP phases and matrix on the morphologies of TCP phases in Ni-based single crystal superalloys. Materials Characterization, 2022, 183, 111609.	1.9	10
2	Liquid-phase scanning electron microscopy for single membrane protein imaging. Biochemical and Biophysical Research Communications, 2022, 590, 163-168.	1.0	3
3	Dynamic mechanisms of strengthening and softening of coherent twin boundary via dislocation pile-up and cross-slip. Materials Research Letters, 2022, 10, 539-546.	4.1	15
4	Simultaneously enhanced oxidation resistance and mechanical properties in a novel lightweight Ti2VZrNb0.5Al0.5 high-entropy alloy. Science China Materials, 2022, 65, 2842-2849.	3.5	5
5	In situ observation of the effect of the twin boundary orientation on the mechanical properties of single crystalline Ni. Materials and Design, 2022, 219, 110816.	3.3	1
6	Nb/NiTi laminate composite with high pseudoelastic energy dissipation capacity. Materials Today Nano, 2022, 19, 100238.	2.3	2
7	A novel HfNbTaTiV high-entropy alloy of superior mechanical properties designed on the principle of maximum lattice distortion. Journal of Materials Science and Technology, 2021, 79, 109-117.	5.6	83
8	Spinodal-modulated solid solution delivers a strong and ductile refractory high-entropy alloy. Materials Horizons, 2021, 8, 948-955.	6.4	52
9	Timely and atomic-resolved high-temperature mechanical investigation of ductile fracture and atomistic mechanisms of tungsten. Nature Communications, 2021, 12, 2218.	5.8	27
10	Single Tungsten Atom-Modified Cotton Fabrics for Visible-Light-Driven Photocatalytic Degradation and Antibacterial Activity. ACS Applied Bio Materials, 2021, 4, 4345-4353.	2.3	8
11	Initial oxidation of Ni-based superalloy and its dynamic microscopic mechanisms: The interface junction initiated outwards oxidation. Acta Materialia, 2021, 215, 116991.	3.8	27
12	Direct observation of the grain boundaries acting as dislocation sources in nanocrystalline platinum. Materials Characterization, 2021, 181, 111493.	1.9	7
13	Effect of Al content on the thermal oxidation behaviour of AlHfMoNbTi high-entropy alloys analysed by in situ environmental TEM. Corrosion Science, 2021, 191, 109711.	3.0	19
14	Hierarchical grain size and nanotwin gradient microstructure for improved mechanical properties of a non-equiatomic CoCrFeMnNi high-entropy alloy. Journal of Materials Science and Technology, 2021, 92, 195-207.	5.6	68
15	Oxygen changes crack modes of Ni-based single crystal superalloy. Materials Research Letters, 2021, 9, 531-539.	4.1	7
16	"Lattice Strain Matchingâ€â€Enabled Nanocomposite Design to Harness the Exceptional Mechanical Properties of Nanomaterials in Bulk Forms. Advanced Materials, 2020, 32, e1904387.	11.1	13
17	Structural evolution of topologically closed packed phase in a Ni-based single crystal superalloy. Acta Materialia, 2020, 185, 233-244.	3.8	35
18	Characterization of topologically close-packed phases and precipitation behavior of P phase in a Ni-based single crystal superalloy. Intermetallics, 2020, 125, 106887.	1.8	18

#	Article	IF	CITATIONS
19	Multidimensional microscopic investigation of oxidation-induced hollow cavities in a Co–Al–W–Ti–Ta alloy nanotip by electron tomography. Journal of Alloys and Compounds, 2020, 848, 156243.	2.8	1
20	Investigations of EGFR configurations on tumor cell surface by high-resolution electron microscopy. Biochemical and Biophysical Research Communications, 2020, 532, 179-184.	1.0	2
21	A comparative study of rafting mechanisms of Ni-based single crystal superalloys. Materials and Design, 2020, 196, 109097.	3.3	9
22	Defects and Their Elemental Distributions in a Crept Co-Al-W-Ti-Ta Single Crystal Superalloy. Crystals, 2020, 10, 908.	1.0	1
23	Atomistic Mechanism of Stress-Induced Combined Slip and Diffusion in Sub-5 Nanometer-Sized Ag Nanowires. ACS Nano, 2019, 13, 8708-8716.	7.3	37
24	Ultrahigh Photocatalytic Rate at a Singleâ€Metalâ€Atomâ€Oxide. Advanced Materials, 2019, 31, e1903491.	11.1	53
25	First-principles investigations on structural stability, elastic and electronic properties of Co ₇ M ₆ (M= W, Mo, Nb) Âμ phases. Molecular Simulation, 2019, 45, 752-758.	0.9	20
26	Effect of pre-straining treatment on high temperature creep behavior of Ni-based single crystal superalloys. Materials and Design, 2019, 167, 107633.	3.3	12
27	Intergrowth of P phase with Laves phase C36 in the high Mo-containing nickel-base single crystal superalloy. Materials Research Express, 2019, 6, 046528.	0.8	1
28	Microstructural and compositional design of Ni-based single crystalline superalloys ― A review. Journal of Alloys and Compounds, 2018, 743, 203-220.	2.8	288
29	Core structure and strengthening mechanism of the misfit dislocation in nickel-based superalloys during high-temperature and low-stress creep. Journal of Alloys and Compounds, 2018, 743, 372-376.	2.8	11
30	Minimum interface misfit criterion for the precipitation morphologies of TCP phases in a Ni-based single crystal superalloy. Intermetallics, 2018, 94, 55-64.	1.8	31
31	Heterostructure TiO 2 polymorphs design and structure adjustment for photocatalysis. Science Bulletin, 2018, 63, 314-321.	4.3	16
32	Growth twins of R phase in the high Mo-containing nickel-base single crystal superalloy. Materials Research Express, 2018, 5, 126517.	0.8	0
33	Atomic arrangement and formation of planar defects in the μ phase of Ni-base single crystal superalloys. Journal of Alloys and Compounds, 2018, 766, 775-783.	2.8	13
34	In situ atomic scale mechanisms of strain-induced twin boundary shear to high angle grain boundary in nanocrystalline Pt. Ultramicroscopy, 2018, 195, 69-73.	0.8	9
35	Effect of chemical composition on particle morphology of topologically close-packed precipitates in a Ni-based single crystal superalloy. Scripta Materialia, 2018, 157, 100-105.	2.6	25
36	A modification on Brook formula in calculating the misfit of Ni-based superalloys. Materials and Design, 2017, 126, 12-17.	3.3	21

Shengcheng Mao

#	Article	IF	CITATIONS
37	Site preference of metallic elements in M23C6 carbide in a Ni-based single crystal superalloy. Materials and Design, 2017, 129, 9-14.	3.3	32
38	In-situ investigation of dislocation tangle–untangle processes in small-sized body-centered cubic Nb single crystals. Materials Letters, 2017, 198, 16-18.	1.3	4
39	Size effect on the deformation mechanisms of nanocrystalline platinum thin films. Scientific Reports, 2017, 7, 13264.	1.6	20
40	Shearing mechanisms of stacking fault and anti-phase-boundary forming dislocation pairs in the γ′ phase in Ni-based single crystal superalloy. Journal of Alloys and Compounds, 2017, 724, 287-295.	2.8	52
41	Elemental preference and atomic scale site recognition in a Co-Al-W-base superalloy. Scientific Reports, 2017, 7, 17240.	1.6	11
42	Tailoring perpendicular magnetic anisotropy with graphene oxide membranes. RSC Advances, 2017, 7, 52938-52944.	1.7	3
43	Response to "Comments on â€~Selective evolution of secondary γ′ precipitation in a Ni-based single crystal superalloy both in the γ matrix and at the dislocation nodes'― Scripta Materialia, 2017, 129, 104-106.	2.6	2
44	Characterization and formation of $ f \hat{l}^3$ interface in Ni-based single crystal superalloys. Materials Research Express, 2017, 4, 116512.	0.8	3
45	MEMS Device for Quantitative In Situ Mechanical Testing in Electron Microscope. Micromachines, 2017, 8, 31.	1.4	8
46	Cloning Nacre's 3D Interlocking Skeleton in Engineering Composites to Achieve Exceptional Mechanical Properties. Advanced Materials, 2016, 28, 5099-5105.	11.1	119
47	Selective evolution of secondary γ′ precipitation in a Ni-based single crystal superalloy both in the γ matrix and at the dislocation nodes. Acta Materialia, 2016, 116, 343-353.	3.8	50
48	Effect of lattice misfit on the evolution of the dislocation structure in Ni-based single crystal superalloys during thermal exposure. Acta Materialia, 2016, 120, 95-107.	3.8	79
49	Reveal the size effect on the plasticity of ultra-small sized Ag nanowires with in situ atomic-scale microscopy. Journal of Alloys and Compounds, 2016, 676, 377-382.	2.8	13
50	Strongly enhanced ultraviolet emission of an Au@SiO ₂ /ZnO plasmonic hybrid nanostructure. Nanoscale, 2016, 8, 4030-4036.	2.8	18
51	Evolution of microstructure and mechanical properties of a dissimilar aluminium alloy weldment. Materials and Design, 2016, 90, 230-237.	3.3	29
52	Revealing ultralarge and localized elastic lattice strains in Nb nanowires embedded in NiTi matrix. Scientific Reports, 2015, 5, 17530.	1.6	20
53	Synthesis of layered double hydroxides/graphene oxide nanocomposite as a novel high-temperature CO2 adsorbent. Journal of Energy Chemistry, 2015, 24, 127-137.	7.1	121
54	Kink structures induced in nickel-based single crystal superalloys by high-Z element migration. Journal of Alloys and Compounds, 2015, 618, 750-754.	2.8	13

#	ARTICLE	IF	CITATIONS
55	Luminescence Properties of GaAs Quantum Dot-in-Nanowire Structure for Quantum Photonics. , 2015, , .		0
56	In-situ observation of crack propagation through the nucleation of nanoscale voids in ultra-thin, freestanding Ag films. Materials Science & Engineering A: Structural Materials: Properties, Microstructure and Processing, 2014, 618, 614-620.	2.6	10
57	Identification of the partitioning characteristics of refractory elements in I_f and \hat{I}^3 phases of Ni-based single crystal superalloys based on first principles. Materials Chemistry and Physics, 2014, 147, 483-487.	2.0	7
58	Locality and rapidity of the ultra-large elastic deformation of Nb nanowires in a NiTi phase-transforming matrix. Scientific Reports, 2014, 4, 6753.	1.6	18
59	Structural, electronic and elastic properties of the C14 NbCr2 Laves phase under hydrostatic pressure. Solid State Communications, 2013, 174, 46-49.	0.9	8
60	A Transforming Metal Nanocomposite with Large Elastic Strain, Low Modulus, and High Strength. Science, 2013, 339, 1191-1194.	6.0	241
61	Stress-induced martensitic transformation in nanometric NiTi shape memory alloy strips: An in situ TEM study of the thickness/size effect. Journal of Alloys and Compounds, 2013, 579, 100-111.	2.8	37

First-principles studies of the structural and electronic properties of the C14 Laves phase XCr2(X $\hat{a} \in \infty = \hat{a} \in \infty$ Ti,) Tj ETQq0 0 0 rgBT /Over 10 0.7 eVertices of the C14 Laves phase XCr2(X $\hat{a} \in \infty = \hat{a} \in \infty$ Ti,) Tj ETQq0 0 0 rgBT /Over

63	High resolution transmission electron microscopy studies of σ phase in Ni-based single crystal superalloys. Journal of Alloys and Compounds, 2012, 536, 80-84.	2.8	28
64	EFFECT OF TEMPERATURE ON MICROSTRUCTURE AND NANOINDENTATION MECHANICAL PROPERTIES OF ELECTRODEPOSITED NANO-TWINNED Ni. Jinshu Xuebao/Acta Metallurgica Sinica, 2012, 48, 1342.	0.3	3
65	Crystallographic Study of Superelastic Deformation of Nitinol. Journal of ASTM International, 2009, 6, 1-9.	0.2	2
66	Effect of Cyclic Loading on Apparent Young's Modulus and Critical Stress in Nano-Subgrained Superelastic NiTi Shape Memory Alloys. Materials Transactions, 2006, 47, 735-741.	0.4	24
67	<i>In-Situ</i> TEM Study of the Thickness Impact on the Crystallization Features of a Near Equal-Atomic TiNi Thin Film Prepared by Planar Magnetron Sputtering. Materials Transactions, 2006, 47, 536-539.	0.4	1
68	Selective Phase and Elemental Oxidation on γ/γ' Structure Co-Al-W-Ti-Ta Alloy Nano Lamella by In-Situ Environmental TEM. SSRN Electronic Journal, 0, , .	0.4	0